



Dynamic changes of serum metabolites associated with infection and severity of patients with acute hepatitis E infection

Jian Wu^{1,2} | Yanping Xu¹ | Yubao Cui³ | Mariza Bortolanza⁴ | Minjie Wang¹ | Bin Jiang⁵ | Meina Yan² | Wei Liang² | Yiwen Yao⁴ | Qiaoling Pan¹ | Jinfeng Yang¹ | Jiong Yu¹ | Dawei Wang⁶ | Hongcui Cao^{1,7}  | Lanjuan Li¹ 

¹State Key Laboratory for Diagnosis and Treatment of Infectious Diseases, National Clinical Research Center for Infectious Diseases, The First Affiliated Hospital, Zhejiang University School of Medicine, Hangzhou, China

²Department of Clinical Laboratory, The Affiliated Suzhou Hospital of Nanjing Medical University, Suzhou Municipal Hospital, Gusu School, Nanjing Medical University, Suzhou, China

³Department of Clinical Laboratory, The Affiliated Wuxi People's Hospital of Nanjing Medical University, Wuxi, China

⁴Department of Internal Medicine V-Pulmonology, Allergology, Respiratory Intensive Care Medicine, Saarland University Hospital, Homburg, Germany

⁵Department of Laboratory Medicine, The Central Blood Station of Yancheng City, Yancheng, China

⁶Department of Infectious Diseases, The Second People's Hospital of Yancheng City, Yancheng, China

⁷Zhejiang Provincial Key Laboratory for Diagnosis and Treatment of Aging and Physic-chemical Injury Diseases, Hangzhou, China

Correspondence

Hongcui Cao, State Key Laboratory for the Diagnosis and Treatment of Infectious Diseases, National Clinical Research Center for Infectious Diseases, The First Affiliated Hospital, Zhejiang University School of Medicine, 79 Qingchun Rd, Hangzhou 310003, China.
Email: hccao@zju.edu.cn.

Funding information

National Major Science and Technology Projects of China

Abstract

Dynamic changes in metabolites may affect liver disease progression, and provide new methods for predicting liver damage. We used ultra-performance liquid chromatography–mass spectrometry to assess serum metabolites in healthy controls (HC), and patients with acute hepatitis E (AHE) or hepatitis E virus acute liver failure (HEV-ALF). The principal component analysis, partial least squares discriminant analysis, and discriminant analysis of orthogonal projections to latent structures models illustrated significant differences in the metabolite components between AHE patients and HCs, or between HEV-ALF and AHE patients. In pathway enrichment analysis, we further identified two altered pathways, including linoleic acid metabolism and phenylalanine, tyrosine, and tryptophan biosynthesis, when comparing AHE patients with HCs. Linoleic acid metabolism and porphyrin and chlorophyll metabolism pathways were significantly different in HEV-ALF when compared with AHE patients. The discriminative performances of differential metabolites showed that taurocholic acid, glycocholic acid, glycochenodeoxycholate-3-sulfate, and docosahexaenoic acid could be used to distinguish HEV-ALF from AHE patients. The serum levels of glycocholic acid, taurocholic acid, deoxycholic acid glycine conjugate, and docosahexaenoic acid

Abbreviations: ACLF, acute-on-chronic liver failure; AHE, acute hepatitis E; ALF, acute liver failure; ESI, electrospray ionization; GC-MS, gas chromatography-mass spectrometry; HC, healthy controls; HEV, hepatitis E virus; INR, international normalized ratio; KEGG, Kyoto Encyclopedia of Gene and Genomes; MS, mass spectrometry; OPLS-DA, orthogonal projections to latent structures discriminant analysis; PLS-DA, projections to latent structures-discriminant analysis; SD, standard deviation; SMPDB, small molecule pathway database; UPLC-MS, ultra performance liquid chromatography mass spectrometry; VIP, variable importance in the projection.

Jian Wu, Yanping Xu, and Yubao Cui are contributed equally to this study.

were associated with the prognosis of HEV-ALF patients. Dynamic changes in serum metabolites were associated with AHE infection and severity. The identified metabolites can be used to diagnose and predict the prognosis of HEV-ALF.

KEYWORDS

acute hepatitis E, acute liver failure, diagnose and prognosis, MS, serum metabolites, UPLC

1 | INTRODUCTION

Hepatitis E is an infectious disease of the digestive tract caused by the hepatitis E virus (HEV), and occurs mainly as sporadic cases in developed countries and epidemics in developing countries.^{1,2} Its epidemic characteristics are similar to those of hepatitis A, which is mainly transmitted through the fecal-oral route and has obvious seasonality. Water-type epidemics are the most common, and a few are food-type outbreaks or through daily contact transmission.^{3,4} The majority of acute hepatitis E (AHE) patients are young and middle-aged; pregnant women are more susceptible; and the condition is serious and the mortality rate is high, which ultimately leads to 3000 stillbirths and 55 000 deaths each year.⁵

In the past decade, acute liver failure (ALF) caused by HEV infection has become more common, although HEV infection usually causes acute and self-limiting disease.^{6,7} Wang and Geng⁸ showed that 6.5% of ALF cases in China had evidence of HEV infection. HEV also causes acute or acute-on-chronic liver failure, and the mortality rate can be as high as 67%.⁷ Liver failure (LF) is often manifested as severe impairment or decompensation of liver function. Clinical symptoms usually include abnormal liver metabolism, coagulation dysfunction, jaundice, hepatic encephalopathy, and hepatorenal syndrome.^{9,10} Routinely, the diagnosis of acute infection usually uses enzyme-linked immunoassay to detect serum IgM antibodies; however, the antibody reaction usually occurs after the week of infection, and the detectable amount during the window is negligible.^{11,12} Due to the insufficient effectiveness and sensitivity of screening indicators, the participation of HEV in ALF is often underestimated or ignored.

Metabolomics makes a considerable contribution to related changes in metabolites in disease states, contributing to the development of drug targets and identification of biomarkers.^{13–15} The main techniques currently used for metabolomics are gas chromatography–mass spectrometry and liquid chromatography–mass spectrometry (LC-MS).^{16,17} Due to the deep coverage of metabolites and visual analysis, LC-MS metabolomics has been widely used in biomarker screening research.^{18,19} Several studies have reported the application of metabolomics technology in the study of the pathogenesis of ALF.^{20–22} However, the biomarkers of severity in HEV-related ALF (HEV-ALF) and metabolic changes that occur during progression have not been evaluated.

In this study, we used ultra-performance liquid chromatography–mass spectroscopy (UPLC-MS) to evaluate the metabolic-related changes in different disease states and identify biomarkers related to patients with AHE, which may provide new clues for the development of new biomarkers and treatment strategy for HEV-ALF.

2 | MATERIALS AND METHODS

2.1 | Patients

We enrolled 50 AHE patients, 48 HEV-ALF patients, and 49 healthy controls (HC) who were admitted to the First Affiliated Hospital of Zhejiang University School of Medicine, and the Second People's Hospital of Yancheng City between October 20, 2018 and December 20, 2020. We obtained serum samples when HEV-ALF and AHE patients were enrolled during the acute phase before receiving treatment. We followed up with all the enrolled HEV-ALF patients until February 28, 2021. As in our previous studies,^{23,24} diagnosis of hepatitis E was based on positive serum anti-HEV IgM, and/or >2-fold increase in anti-HEV IgG titer, and/or HEV RNA, in combination with systemic manifestations of acute hepatitis.

The selection criteria for patients with HEV-ALF were based on the King's College criteria,²⁵ which were as follows: (1) evidence of abnormal liver synthetic function (prothrombin activity $\leq 40\%$ or international normalized ratio [INR] ≥ 1.5), jaundice, and hepatic atrophy over a 2-week period; (2) the presence of stage 2 or 3 encephalopathy complicating end-stage disease manifestations; and (3) no chronic liver disease.

The following exclusion criteria were applied: co-infection with hepatitis A virus, hepatitis B virus or other hepatitis viruses; alcoholic liver, fatty liver, and other liver diseases caused by nonviral hepatitis; use of antibiotics, probiotics, prebiotics, or symbiotics during the previous month; active bacterial, fungal, chlamydial, or viral infection; irritable bowel syndrome, inflammatory bowel disease, or other autoimmune diseases; and patients with incomplete data. The present study was endorsed by the Ethics Committee of the First Affiliated Hospital of Zhejiang University School of Medicine (approval number: 2020454).

2.2 | Sample preparation

We collected patient blood samples according to the clinical requirements of biochemical analysis. We collected an additional 2 ml blood sample in a container containing EDTA anticoagulant. After centrifugation at 3000g for 20 min, the plasma samples were aliquoted into fresh Eppendorf tubes and stored at -80°C for subsequent metabolomics analysis. We added 150 μl acetonitrile to a centrifuge tube containing 50 μl thawed serum, vortexed for 5 min, ultrasonically extracted for 10 min, centrifuged at 10 000 rpm for 10 min at 4°C , removed 130 μl supernatant, and added it to a sample

bottle equipped with a liner, and stored for analysis. We also withdrew 20 μ l supernatant from each sample and mixed thoroughly for quality control (QC) samples.

2.3 | UPLC-MS data analysis

The specific procedure for UPLC-MS has been described previously.²⁶ A 2- μ l aliquot was applied to an Acquity UPLC BEH C18 analytical column (2.1 mm \times 100 mm, 1.7 μ m, 130 \AA ; Waters Corp.). The mobile phases were water (A) and acetonitrile (B) with 0.1% formic acid. The flow rate was maintained at 400 μ l/min. The starting composition was 3% B; linearly increased to 98% B, held for 5 min, and then increased to 100% B within 3 min.

Mass spectrometry (MS) was run in both positive and negative modes on a Waters MS equipped with an electrospray ionization source (Waters Quadrupole Time-of-Flight Premier). The corresponding settings of the instrument were: capillary voltage 3 kV and cone voltage was 3.5 kV. The ion source temperature was 120°C, and the dissolved temperature was 450°C. MS data were collected in standard scan mode, ranging from 50 to 1000; the scan time was set to 0.3 s, and the delay between scans was 0.02 s. Nitrogen was principally used as desolvation gas (400 L/h) and cone gas (50 L/h).

2.4 | Data processing

The metabolites were separated by UPLC-MS, and the characteristic peaks obtained by quadrupole time-of-flight MS contained the qualitative information of corresponding substances (retention time, accurate mass, secondary fragment ion, and isotope distribution) and relative quantification information (peak height or peak area). These were the basis for metabolite identification and comparison of differences between different samples or groups. We imported the UPLC-MS raw data into MetaboScape 3.0 software (Bruker Scientific Technology Co. Ltd.) for peak correction, peak extraction, deconvolution, peak alignment, and other processing. The processed data were further imported into SIMCA-P + 14.1 (Umetrics AB, Umea, Sweden) for multivariable statistical analysis. We performed unsupervised principal component analysis (PCA) to evaluate the stability and reconstruction of UPLC-MS data. Discriminant analysis of orthogonal projections to latent structures (OPLS-DA) was performed to identify more sample categories and a predictive model metabolomics model. The selection of differential metabolites was based on the variable importance in projection (VIP) of the first principal component of the partial least squares discriminant analysis (PLS-DA) model and the S plot. VIP >1 meant that the identified substances were meaningful for grouping.

2.5 | Identification of metabolites

Using first-level accurate mass, retention time, isotope peak information, and MS/MS fragment ions as the qualitative basis, the

extracted characteristic peaks were compared with the Human Metabolome Database (HMDB, <http://hmdb.ca/>) to identify metabolites. We used network metabolic pathway databases such as Kyoto Encyclopedia of Genes and Genomes (KEGG) and the Small Molecule Pathway Database (SMPDB) to analyze specific metabolic enrichment pathways and explain the physiological significance and pathological mechanisms of potential markers.

2.6 | HEV-specific antibody detection

All serum samples were tested for the presence of anti-HEV IgM and IgG antibodies using a commercially available HEV ELISA Kit (Wan-tai). Samples with optical density (OD) > 1.1 were considered positive. Samples with OD \leq 1.1 were considered negative.

2.7 | HEV RNA detection

HEV RNA was tested by means of internally controlled quantitative real-time reverse transcription polymerase chain reaction (RT-PCR) as described previously.²⁴ Total RNA was extracted from serum using the QIAamp Viral RNA Mini Kit (Qiagen). A 137-nucleotide fragment of the HEV open reading frame 2/3 (overlapping area) was amplified using a nested polymerase chain reaction (PCR) and sequenced to identify the genotype.²⁷ The viral infection of each sample was estimated using quantitative PCR according to cycle threshold value using a diagnostic Kit for HEV RNA.

2.8 | Treatment of HEV-ALF patients

Since there is no effective treatment for HEV-ALF, management includes intensive care support after the start of antiviral treatment for HEV infection, which mainly includes: (1) bed rest, light diet, reduce physical consumption and reduce burden on the liver; (2) monitoring vital signs, including blood pressure, pulse, respiratory rate, blood oxygen saturation, urine volume, and so forth; (3) monitoring mental state, including changes in computational power, orientation, verbal dialog, and consciousness; (4) use of liver protecting, enzyme reducing, and yellow removing drugs; (5) use of adrenocortical hormone should be cautious; (6) protection of gastric mucosa and prevention of gastrointestinal bleeding; (7) regularly rechecking liver and kidney function, electrolyte levels, routine blood analysis, coagulation function, arterial blood gas, and inflammatory indexes; (8) paying attention to disinfection and isolation to prevent cross-infection; and (9) strengthening nursing to prevent nosocomial infection.

2.9 | Statistical analysis

The specific data involved in the experiment were analyzed using SPSS 22.0. Data with normal distribution were statistically analyzed

with the mean \pm standard deviation. The independent sample *t* test was used for comparison between two groups; the nonparametric Mann–Whitney *U* test was used for non-normally distributed data. $p < 0.05$ was deemed statistically significant.

3 | RESULTS

3.1 | Characteristics of the enrolled population

The characteristics of the study population are shown in Table 1. There was no obvious difference in baseline characteristics including age, gender, and body mass index between the three groups ($p > 0.05$). There were no pregnant women. The results of genotype sequencing of AHE and HEV-ALF patients focused on type 4 and type 3, which were shown in Table S1. The mean follow-up time of HEV-ALF patients was 4.2 months (range, 1.8–8.6 months). Among all the HEV-ALF patients, 93.8% exhibited only failure in the liver, followed by 10.4% with failure in two organs, and 6.3% with failure in three or more organs. Forty-one HEV-ALF patients recovered after treatment and seven died.

3.2 | Multivariate analysis of the UPLC-MS data

After all human samples were analyzed in the positive and negative ion modes of UPLC-MS, a base peak chromatogram was generated (Figure 1). The chromatograms of AHE and HEV-ALF patients and HCs in positive (Figure 1A,B) and negative (Figure 1C,D) ion modes are shown. It can be seen directly on the

graph that there were obvious differences in the number and intensity of these three groups of peaks. Throughout the test, the stability of the machine was judged by observing the chromatogram of the QC sample. Before starting the test, we continued to inject samples until the chromatograms overlapped, and then started the formal testing of the samples. Through PCA, QC samples were clustered together (Figure 1E,F), and there was no QC deviation out of bounds in the whole process. It could be judged that the stability and repeatability of the instrument were good, and the data of this batch of samples were reliable.

3.3 | Metabolomics profiles and multivariate data analyses between HC and AHE groups

After the raw data were pre-processed, the UPLC-MS data were used for multivariate statistical analysis using SIMCA-P + 14.1 software. To establish the influence of HEV on the body's metabolism, both HC and AHE serum metabolomics were measured. Through comparison with the HMDB database, 33 different metabolites were identified in the two groups (Table S2). The metabolomic profiles in two groups were evaluated with PCA and PLS-DA score plots in both positive and negative ion modes (Figure 2). PCA was established for all samples except the QC group in positive (Figure 2A) and negative (Figure 2B) ion modes. The HC and AHE samples could be clearly distinguished, indicating that there was an apparent difference in the metabolic spectrum between the two groups and liver injury may have been accompanied by changes in metabolism. At the same time, we established the PLS-DA model of the two groups of samples. The

TABLE 1 Baseline characteristics of the study population

Variables	HC group (n = 49)	AHE group (n = 50)	HEV-ALF group (n = 48)	<i>p</i> (HC vs. AHE)	<i>p</i> (AHE vs. HEV-ALF)
Age (years)	50.94 \pm 15.96	54.26 \pm 13.60	53.67 \pm 12.82	0.268	0.825
Gender (M/F)	27/22	31/19	25/23	0.486	0.321
BMI	22.08 (20.98–23.44)	21.96 (20.20–23.59)	22.02 (19.36–23.43)	0.649	0.765
WBC ($10^9/L$)	6.3 (5.0–7.9)	5.9 (4.6–8.0)	6.6 (4.7–9.4)	0.312	0.313
ALB (g/L)	45.47 \pm 5.43	36.52 \pm 4.87	30.06 \pm 5.24	<0.001	<0.001
ALT (U/L)	32 (17–43)	251 (96–724)	66 (37–150)	<0.001	<0.001
AST (U/L)	30 (18–38)	124 (63–213)	98 (44–178)	<0.001	0.328
PLT ($\times 10^9/L$)	197 (155–232)	201 (166–266)	64 (37–109)	0.320	<0.001
TBIL ($\mu\text{mol/L}$)	8.9 (5.2–13.6)	25.0 (19.0–95.6)	227.3 (58.8–424.0)	<0.001	<0.001
DBIL ($\mu\text{mol/L}$)	4.4 (3.4–5.6)	16.6 (12.4–83.6)	163.2 (35.8–296.2)	<0.001	<0.001
UREA (mmol/L)	5.25 (3.92–6.52)	4.78 (3.69–6.38)	9.66 (5.40–15.51)	0.526	<0.001
PT (s)	12.40 (11.65–12.75)	17.15 (13.52–18.70)	21.25 (16.42–26.58)	<0.001	<0.001

Abbreviations: AHE, acute hepatitis E; ALB, albumin; ALF, acute liver failure; ALT, alanine aminotransferase; AST, aspartate aminotransferase; BMI, body mass index; DBIL, direct bilirubin; HC, healthy controls; HEV, hepatitis E virus; PLT, platelets; PT, prothrombin; TBIL, total bilirubin; UREA, urea nitrogen; WBC, white blood cell.

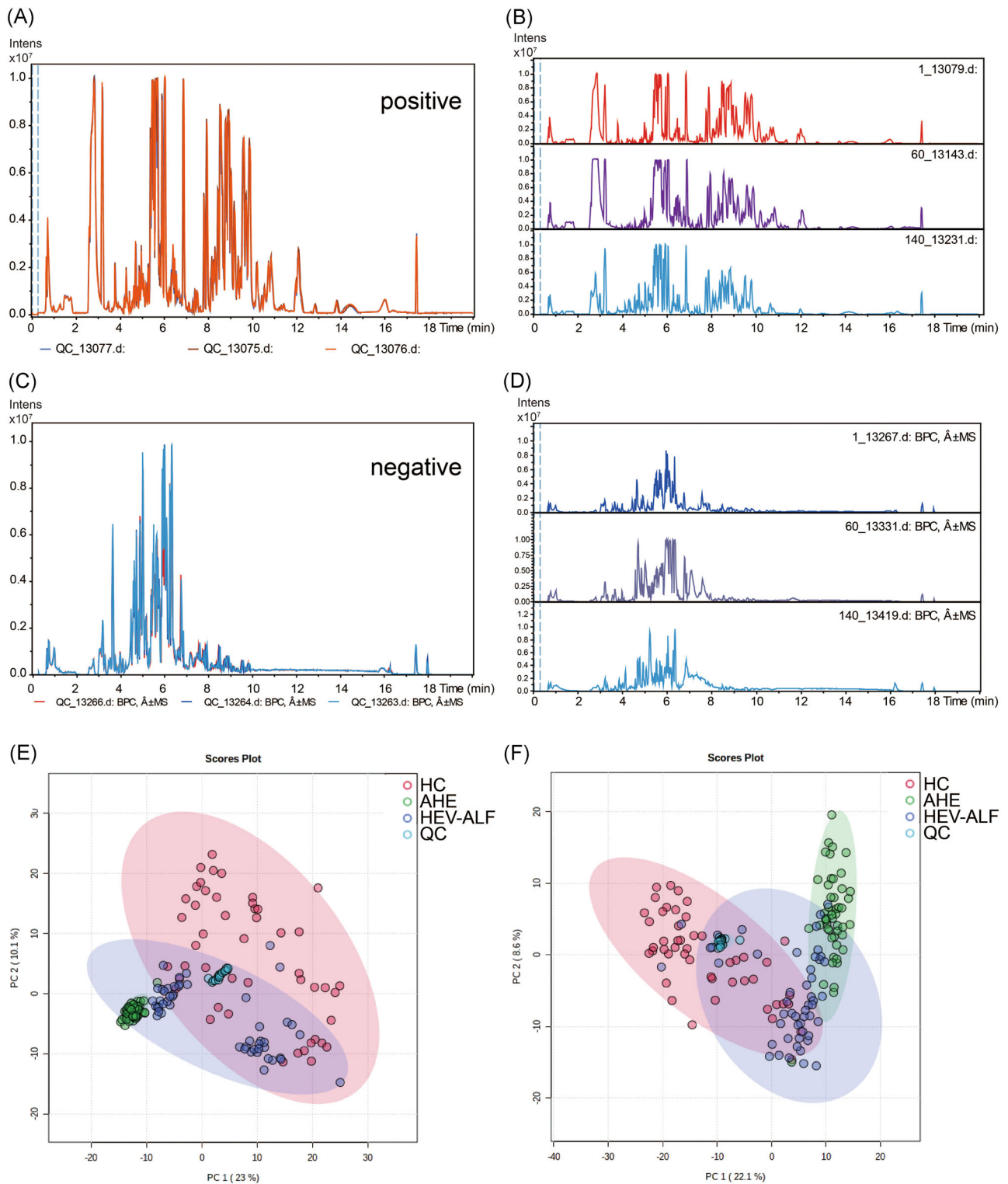


FIGURE 1 Metabolomic profiling by ultra-performance liquid chromatography–mass spectroscopy (UPLC-MS). UPLC-MS total ion chromatograms chromatogram generated by three injections in (A) positive ion spectrum (ES⁺) mode and (C) negative ion spectrum (ES⁻) mode. Three groups of representative base peak chromatogram (BPC) were obtained in (B) ES⁺ mode and (D) ES⁻ mode. Unsupervised principal component analysis score plots in positive (E) and negative (F) ion mode. The quality control (QC) samples (blue) showed tight clusters, indicating that the UPLC-MS method existed in high stability and repeatability. AHE, acute hepatitis E; HC, healthy controls; HEV-ALF, hepatitis E virus acute liver failure

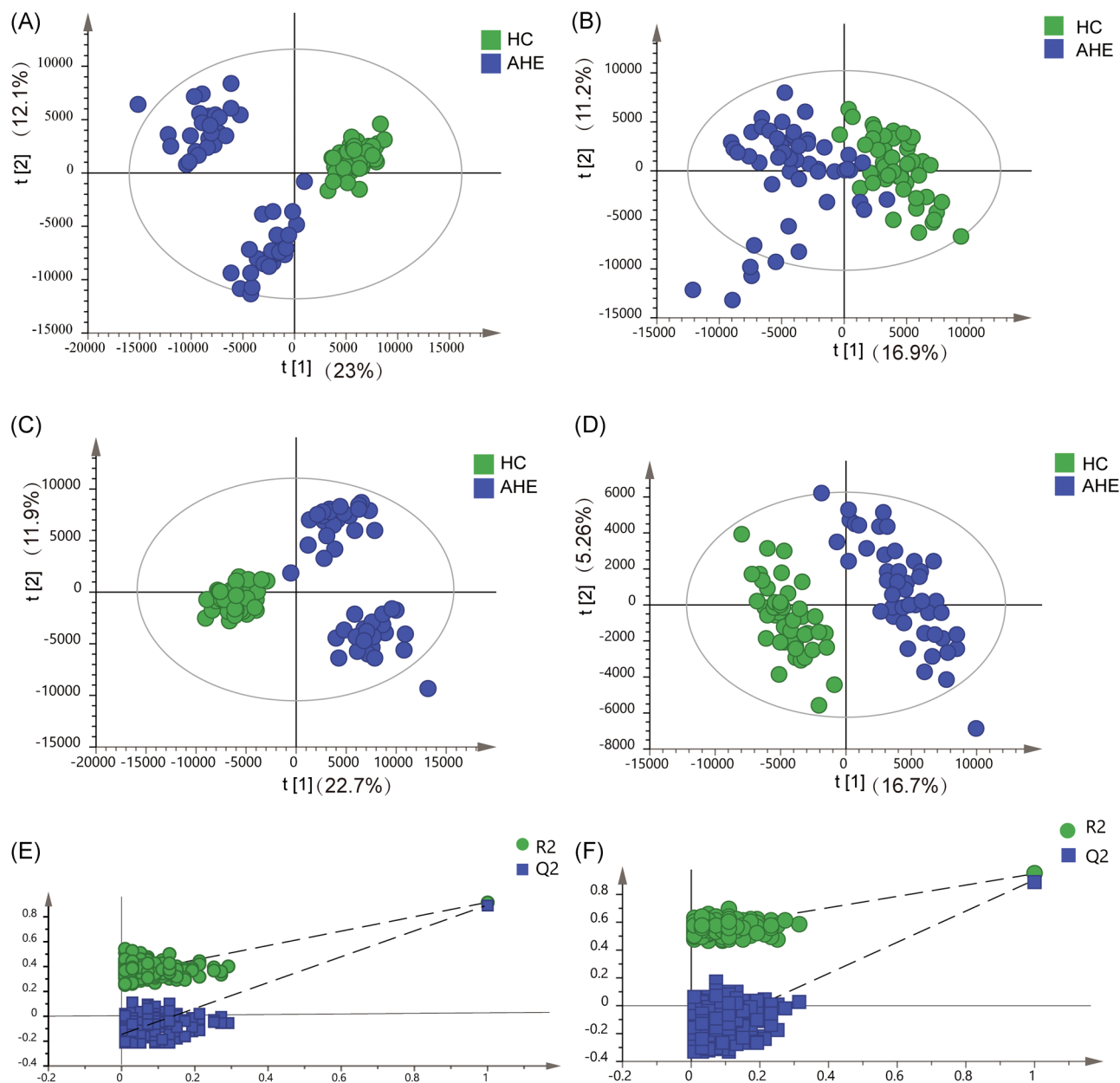


FIGURE 2 Metabolomics diverse data analysis of HC and AHE groups in positive and negative ion modes. principal component analysis model diagrams based on metabolites identified by ultra-performance liquid chromatography–mass spectroscopy (UPLC-MS) in ES⁺ mode (A) and ES⁻ mode (B) in healthy controls (HC) and acute hepatitis E (AHE) groups. Partial least squares discriminant analysis (PLS-DA) model diagrams based on metabolites identified by UPLC-MS in ES⁺ mode (C) and ES⁻ mode (D). (E) Perform 200 permutation tests on the PLS-DA positive ion model, indicating that the model was not over-fitting ($R^2 = [0.0, 0.337]$, $Q^2 = [0.0, -0.145]$). (F) Perform 200 permutation tests on the PLS-DA negative ion model, indicating that the model was not over-fitting ($R^2 = [0.0, 0.53]$, $Q^2 = [0.0, -0.21]$). $N = 50$ per group

samples of the two groups could be distinguished in both positive (Figure 2C) and negative (Figure 2D) ion modes, indicating that there was a difference in the metabolic spectrum between the two groups. The PLS-DA model was subjected to 200 replacement tests, $Q^2 = -0.145$ in the positive ion mode (Figure 2E), and $Q^2 = -0.21$ in the negative ion mode (Figure 2F), $Q^2 < 0.05$, indicating that the model was not overfitting.

3.4 | Metabolomics profiles and multivariate data analyses between AHE and HEV-ALF groups

Through comparison with the HMDB database, 32 different metabolites were identified in the AHE and HEV-ALF groups (Table S3). The metabolomic profiles in the two groups were evaluated with PLS-DA and OPLS-DA score plots in positive

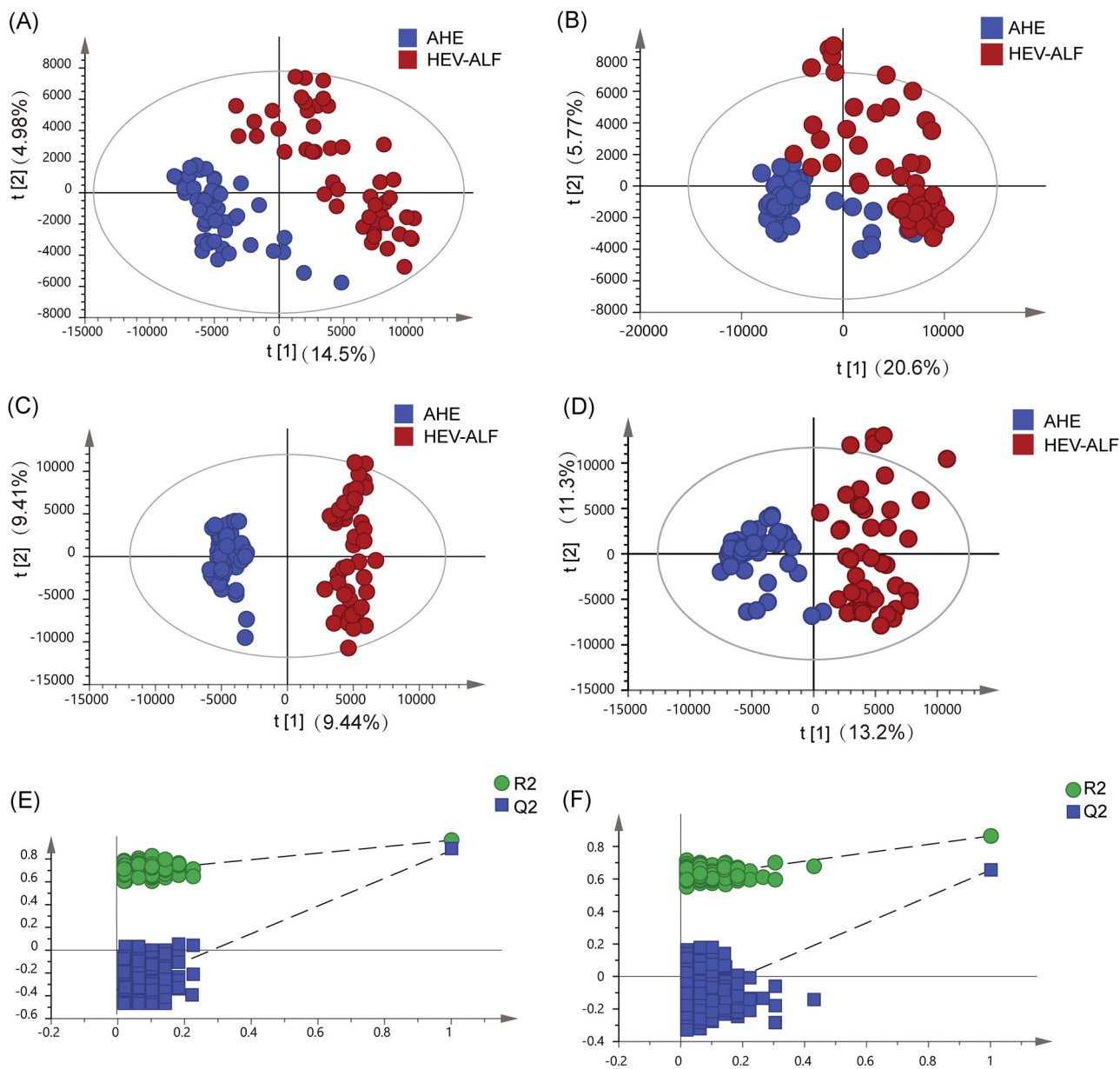


FIGURE 3 Metabolomics diverse data analysis of acute hepatitis E (AHE) and hepatitis E virus acute liver failure (HEV-ALF) groups in positive and negative ion modes. Partial least squares discriminant analysis (PLS-DA) model diagrams based on metabolites identified by ultra-performance liquid chromatography–mass spectrometry (UPLC-MS) in ES⁺ mode (A) and ES[−] mode (B) in AHE and HEV-ALF groups. Orthogonal projections to latent structures discriminant analysis model diagrams based on metabolites identified by UPLC-MS in ES⁺ mode (C) and ES[−] mode (D). (E) Perform 200 permutation tests on the PLS-DA positive ion model, indicating that the model was not over-fitting ($R^2 = [0.0, 0.68]$, $Q^2 = [0.0, -0.347]$). (F) Perform 200 permutation tests on the PLS-DA negative ion model, indicating that the model was not over-fitting ($R^2 = [0.0, 0.606]$, $Q^2 = [0.0, -0.158]$). $N = 50$ per group

(Figure 3A,C) and negative (Figure 3B,D) ion modes. The OPLS-DA two-dimensional diagram shows sample separation between AHE and HEV-ALF groups in positive (Figure 3C) and negative (Figure 3D) ion modes. Metabolites were derived from the OPLS-DA model according to $VIP > 1$ and a significant difference ($p < 0.05$) between any two groups, which showed that liver damage may be accompanied by metabolic changes. Furthermore,

the R^2 -intercept of serum metabolites was 0.68 and 0.606 in the positive (Figure 3E) and negative (Figure 3F) ion modes, respectively. $Q^2 = -0.347$ in positive ion mode and -0.158 in negative ion mode suggested that the PLS-DA model had no risk of overfitting. These results indicated a significant difference ($p < 0.05$) between AHE and HEV-ALF groups. Those metabolites with $VIP > 1$ were selected as candidate biomarkers of HEV-ALF.

3.5 | Metabolomics profiles and multivariate data analyses of all groups

PCA is often used for dimensionality reduction of high-dimensional data, and can be used to extract the main feature components of data. PCA diagrams of all tested specimens (QC, AHE, HEV-ALF, and HC) are shown in positive (Figure 4A) and negative (Figure 4B) ion modes. The QC group was gathered together in the two ion modes to prove the reliability of metabolome data in this experiment. In the PCA scoring chart, no obvious separation trend was observed in the AHE and HEV-ALF groups, but the separation trend of the HC group from these two groups in the positive ion mode was obvious (Figure 4A). PLS-DA and OPLS-DA diagrams characterized the metabolic profile characteristics of different groups in positive (Figure 4C,E) and negative (Figure 4D,F) ion mode. The HC group was clearly distinguished from the other two groups (Figure 4E,F).

3.6 | Correlation and pathway analysis of differential metabolites

Through pathway enrichment analysis, we preliminarily analyzed the biological processes or signaling pathways in which different metabolites may participate. Thirteen pathways were relevant to the crucial metabolites between HC and AHE groups (Figure 5A) and 12 pathways were relevant to the crucial metabolites between AHE and HEV-ALF groups (Figure 5B). In the pathway analysis diagram, the horizontal axis represents the pathway influence value of the pathway analysis, and the vertical axis is the $-\log_{10}(p)$ value of the pathway enrichment analysis. These pathways were related to the metabolism of linoleic acid, phenylalanine, tyrosine and tryptophan biosynthesis, arachidonic acid, unsaturated fatty acids, glycerophospholipid, taurine and hypotaurine, primary bile acid, and ether lipid. Linoleic acid metabolism ($p = 0.00001$) and phenylalanine, tyrosine, and tryptophan biosynthesis ($p = 0.043$) pathways enabled discrimination of HC and AHE groups (Figure 5A). Linoleic acid metabolism ($p = 0.00124$) and porphyrin and chlorophyll metabolism ($p = 0.045$) pathways enabled discrimination of AHE and HEV-ALF groups (Figure 5B).

Correlation between serum crucial metabolite levels and liver phenotypes was determined (Figure 6). The darker color of the circle in the figure indicated that there was a clear correlation between these biomarkers. Aspartate transaminase (AST) and alanine transaminase (ALT) assumed a negative correlation with most metabolites, although there was a positive correlation between AST and ALT in both positive and negative ion modes, suggesting liver damage caused by high levels of ALT and AST suppressed the expression of other metabolites. Palmitic amide and octadecanamide promoted each other strongly and had the highest correlation. On the contrary, another metabolite, lecithin, demonstrated a negative correlation with lysoplasmenylcholine, C18:1 sphingomyelin, and phenylalanyl-phenylalanine (Figure 6A). In negative ion mode, glycocholic acid

showed a positive correlation with bilirubin, deoxycholic acid glycine conjugate, and taurocholic acid (Figure 6B).

3.7 | Discriminative and prognostic performances of differential metabolites in patients with hepatitis E infection

To assess the discriminative performances of differential metabolites between AHE and HEV-ALF groups, receiver operating characteristic analysis was performed, and the area under the curve (AUC) of the important difference metabolites in the positive and negative ion modes was calculated. Metabolites with $AUC > 0.80$ were selected as key biomarkers. We observed that taurocholic acid, glycocholic acid, glycochenodeoxycholate-3-sulfate, and docosahexaenoic acid could be used to differentiate patients with HEV-ALF from those with AHE with an AUC of 0.84, 0.85, 0.82, and 0.81, respectively (Figures S1 and S2).

Kaplan–Meier analysis was used to evaluate whether altered metabolites were related to the prognosis of HEV-ALF. We invented that serum levels of glycocholic acid, taurocholic acid, and deoxycholic acid glycine conjugate were more abundant in dead patients, while docosahexaenoic acid was more abundant in surviving patients (all $p < 0.05$; Figure S3).

4 | DISCUSSION

In recent years, there have been more reports of HEV-ALF, but the identification of related metabolites has not been performed, and diagnostic markers for HEV-ALF are still rare. The central goal of clinical treatment of patients with LF is to screen for important biomarkers for diagnosis, treatment, and prognosis of the disease based on the causes and clinical manifestations of various complications.²⁸ In our study, we used UPLC-MS, which is used for non-volatile fatty acids, phospholipids, and bile acids, to assess the serum metabolites of patients with AHE. UPLC-MS data showed the corresponding separation between groups and tight clusters within each group, highlighting the high sensitivity and strong coverage of this method.

In this study, the PCA, PLS-DA, and OPLS-DA models illustrated significant differences in the detected serum metabolites between AHE patients and HCs, and between HEV-ALF and AHE patients. Comparison among the three groups revealed dynamic changes accompanied with the occurrence and development of the disease. Among the 33 identified metabolites, 14 in positive ion mode were observed when comparing between AHE and HC groups. Similarly, among the 32 identified metabolites, 17 in positive ion mode were observed when comparing between AHE and HEV-ALF groups. On the whole, amino acids, and bile acids were the two most abundant metabolites. Bilirubin, taurocholic acid, glycocholic acid, lecithin, and deoxycholic acid glycine conjugate showed different results in the two groups (highly expressed levels in the HEV-ALF groups and less

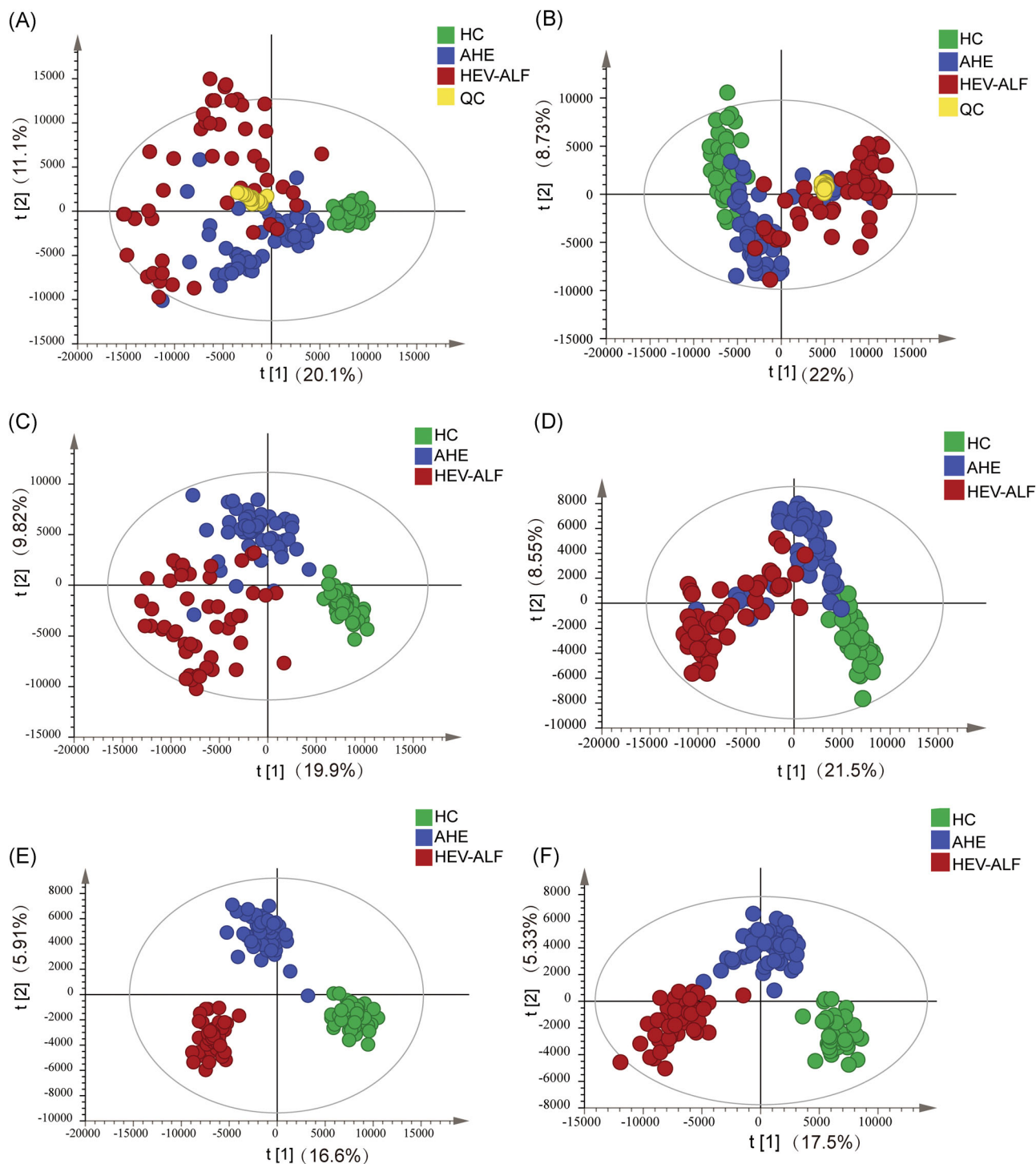


FIGURE 4 Metabolomics profiles and multivariate data analyses in positive and negative ion modes. Principal component analysis model diagrams with quality control (QC) samples of serum metabolites by ultra-performance liquid chromatography–mass spectroscopy (UPLC-MS) in ES⁺ mode (A) and ES⁻ mode (B). Partial least squares discriminant analysis (PLS-DA) score plots without QC samples of serum metabolites in ES⁺ mode (C) and ES⁻ mode (D). Orthogonal projections to latent structures discriminant analysis model diagrams without QC samples of serum metabolites in ES⁺ mode (E) and ES⁻ mode (F). In healthy controls (HC), acute hepatitis E (AHE), and hepatitis E virus acute liver failure (HEV-ALF) groups, $n = 50$ in each group

expression in the AHE group), so it was of importance for studying the mechanism of disease progression.

Necrotic liver cells can release amino acids into peripheral blood during liver injury, causing a significant increase in amino acidemia. In

this way, elevated amino acid levels in ALF are due to impaired liver function, decreased protein synthesis, and activated protein degradation.²⁹ The levels of combined bile acids such as taurocholic acid, deoxycholic acid glycine conjugate increased after ALF, which

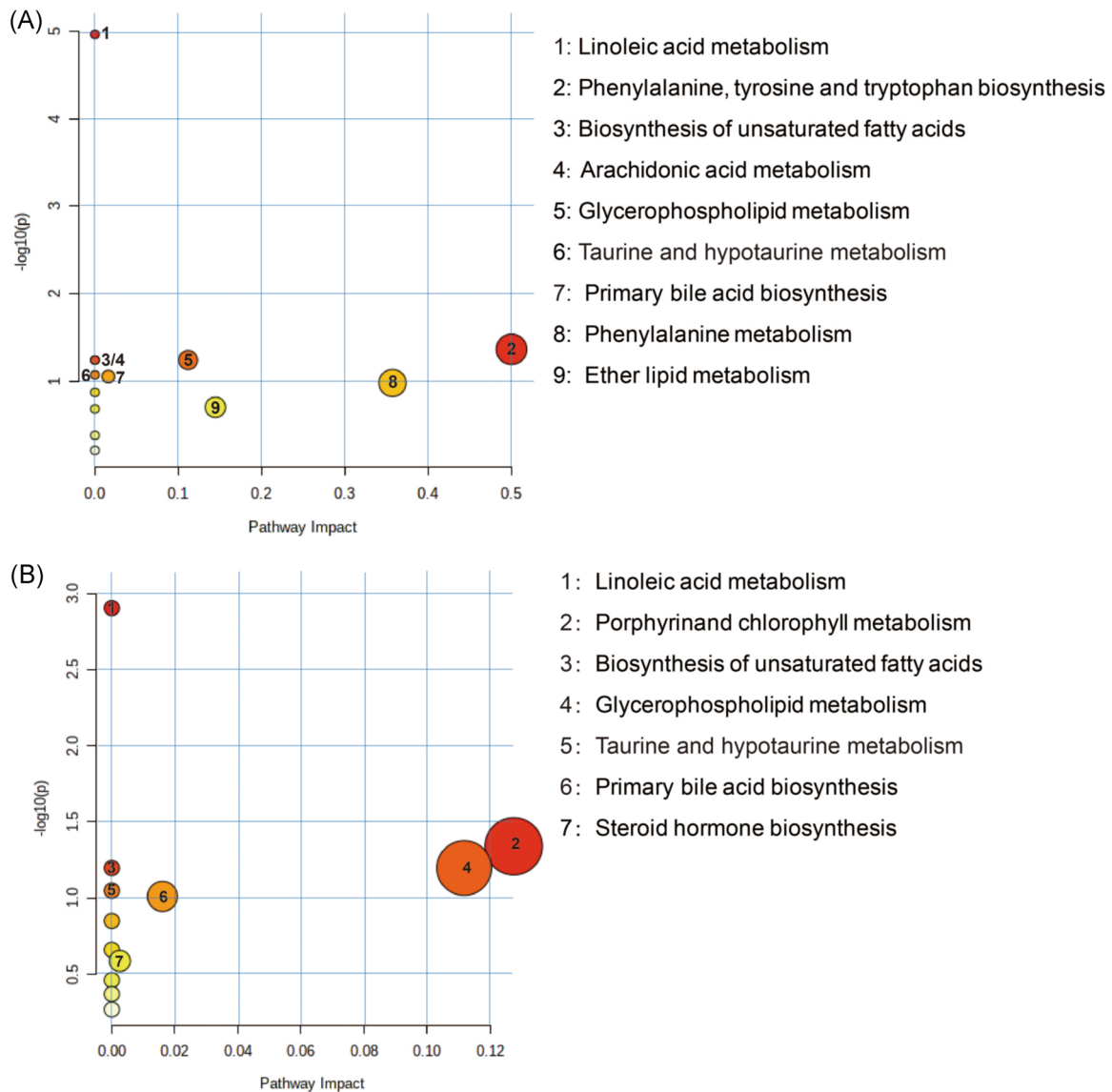


FIGURE 5 Metabolic pathway analysis of healthy controls (HC), acute hepatitis E (AHE), and hepatitis E virus acute liver failure (HEV-ALF) groups. (A) Analysis of metabolic pathways with significant differences between the HC and AHE groups. (B) Analysis of metabolic pathways with significant differences between AHE and HEV-ALF groups. Generally, the higher the pathway impact value and the $-\log(p)$ value, the larger the circle and the darker color in the figure, indicating that this approach had a large influence

were consistent with the changes in AST and ALT levels. In normal conditions, the level of bile acids in the peripheral blood is low due to the intestinal–hepatic circulation. Nevertheless, liver cell damage disrupts the absorption and excretion of the liver, leading to an increase in combined bile acids in serum.³⁰ This leads to apoptosis and necrosis of liver cells and might cause further damage.^{31,32}

In the pathway enrichment analysis, we identified two altered pathways of linoleic acid metabolism and phenylalanine, tyrosine, and tryptophan biosynthesis when comparing AHE patients with HCs. Linoleic acid metabolism and porphyrin and chlorophyll metabolism pathways were significantly different in HEV-ALF and AHE patients. Two of the important pathways were related to amino acid metabolism, indicating that there was a corresponding connection

between amino acid metabolism and AHE. Some previous studies have revealed that there is an association between amino acid metabolic disorders and liver disease.³³ In our study, amino acids were expressed diversely in the serum, and they were the most abundant differential metabolites. Linoleic acid is one of the essential fatty acids, which can maintain lower expression of plasma low-density lipoprotein cholesterol.³⁴ Khosla and Fungwe³⁵ provided information that increasing the intake of linoleic acid has a significant beneficial effect on the progression of atherosclerosis. Phenylalanine is one of the essential amino acids, and the activity level of the phenylalanine metabolism pathway may reflect the synthesis and breakdown state of the systematic protein, and together with tyrosine, it synthesizes important biomolecules and takes part in carbohydrate and fat

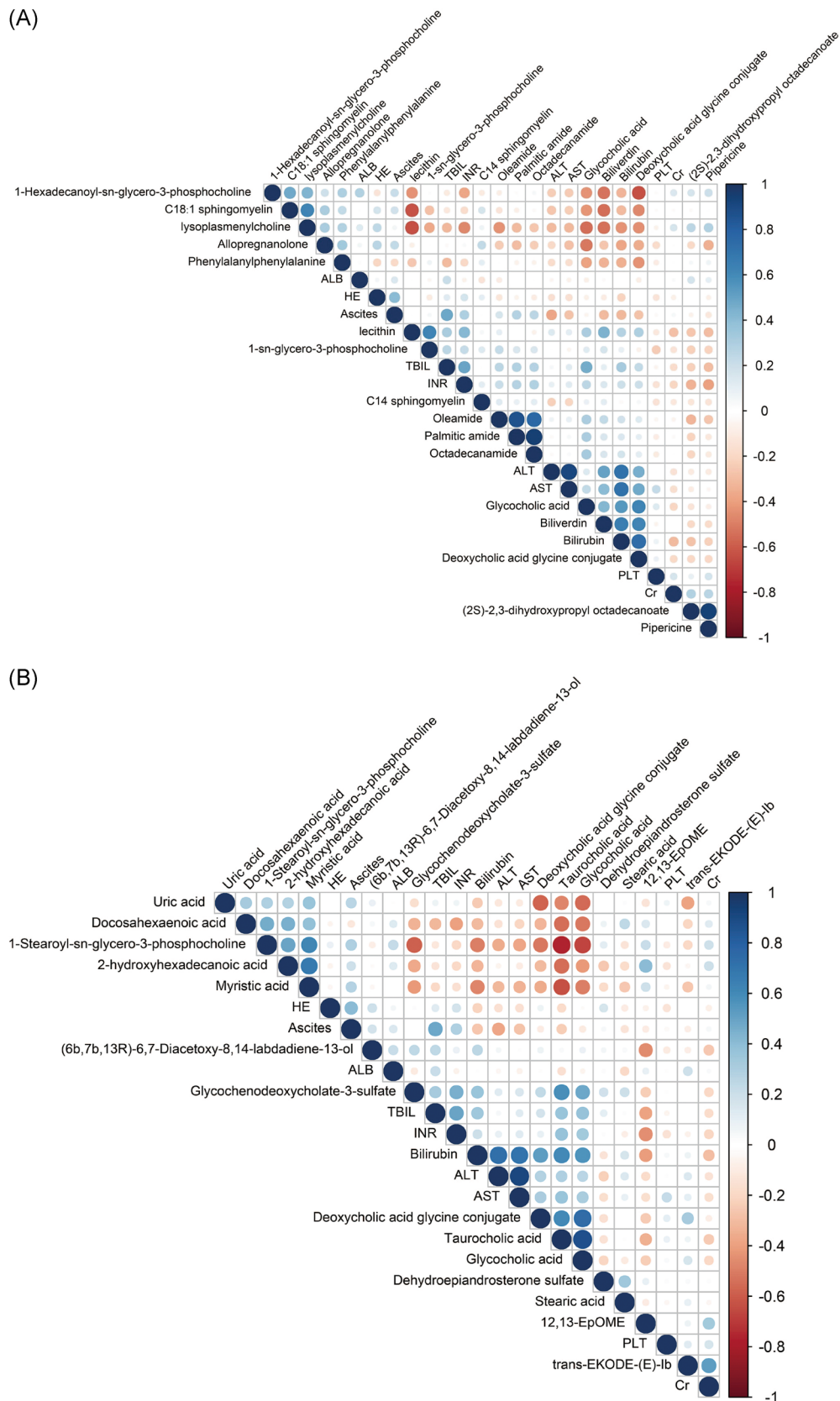


FIGURE 6 Correlation analysis of differential metabolites between acute hepatitis E (AHE) and hepatitis E virus acute liver failure (HEV-ALF) groups. Spearman rank-based correlation analysis between serum metabolite levels and liver phenotypes of AHE and HEV-ALF groups in ES⁺ mode (A) and ES⁻ mode (B). According to the statistical test, the white area represented no correlation between the different metabolites ($p > 0.05$). The blue circles represented the mutual promotion between different metabolites, and the red circles represented the inhibitory relationship between different metabolites ($p < 0.05$). ALT, alanine transaminase; AST, aspartate transaminase; INR, international normalized ratio

metabolism.³⁶ Porphyrin and its derivative compounds are widely present in vital organelles related to energy transfer, and play a key role in blood cells carrying oxygen for respiration.³⁷

In the past few years, researchers have found that acetic acid, sorbitol, D-lactic acid, hexanoic acid, L-naphthalenamine, butanoic acid, phosphoric acid, D-glucitol, and glucose concentration in the serum samples of patients with HBV were the strongest segregation between cirrhosis group and non-cirrhosis group.³⁸ Another study has revealed that hepatitis C is consistent with impaired glucose uptake, glycolysis, and pentose phosphate pathway metabolism, with the tricarboxylic acid pathway fueled by branched-chain amino acids feeding gluconeogenesis and the hepatocellular loss of glucose, which most probably contributes to hyperglycemia.³⁹

An accurate understanding of the activity of HEV helps us to improve the treatment plan for patients with LF. Nevertheless, there is currently a lack of convenient and sensitive laboratory markers to assess the activity of AHE. The discriminative performances of differential metabolites showed that taurocholic acid, glycocholic acid, glycochenodeoxycholate-3-sulfate, and docosahexaenoic acid could be used to distinguish patients with HEV-ALF from those with AHE. The serum levels of glycocholic acid, taurocholic acid, deoxycholic acid glycine conjugate, and docosahexaenoic acid were associated with the prognosis of HEV-ALF patients.

As far as we know, this is the first study reporting serum metabolomics in patients with HEV infection. The investigation of diagnostic and disease-active biomarkers may help diagnose and determine the clinical stage of the disease. Many liver-related metabolomics studies only recognized the different metabolites between each group. The levels of linoleic acid and bile acid were significantly increased in the liver injury group. We could consider reducing the levels of these metabolites. However, our research had several limitations. The number of samples used was small, especially owing to the problem of collecting samples from patients with progressive HEV-ALF. Our study did not investigate the serum metabolomics in different stages of HEV infection (such as chronicity). HEVs with different genotypes were not studied. It is necessary to conduct further longitudinal studies on a large sample of patients to study the differential metabolites at different phases of the disease.

5 | CONCLUSION

The dynamic changes in serum metabolites were associated with AHE infection and severity. The identified changes in serum metabolite levels can be used to diagnose and predict the prognosis of HEV-ALF, which may provide new clues for the development of new biomarkers and treatment strategies for HEV-ALF.

ACKNOWLEDGMENT

This study was supported by the major national science and technology projects on infectious diseases (No. 81790630).

CONFLICTS OF INTEREST

The authors declare no conflicts of interest.

ETHICS STATEMENT

The protocol for the present study was endorsed by the Ethics Committee of the First Affiliated Hospital of Zhejiang University School of Medicine (approval number: 2020454). Informed consent was obtained from all participants or their families.

AUTHOR CONTRIBUTION

Hongcui Cao is the guarantor of this study; Jian Wu, Yanping Xu, and Yubao Cui experimental design, acquisition of data, analysis and interpretation of data, drafting of the manuscript, statistical analysis; Jian Wu, Yanping Xu, Qiaoling Pan, Minjie Wang, and Mariza Bortolanza conducted the main experiments; Meina Yan, Wei Liang, Dawei Wang, Jinfeng Yang, and Jiong Yu collected serum and completed the follow-up; Yiwen Yao, and Bin Jiang: acquisition of data, statistical analysis, critical revision of the manuscript; Hongcui Cao and Lanjuan Li obtained financial support for this study, study concept and design, study supervision, and critical revision of the manuscript for important intellectual content.

DATA AVAILABILITY STATEMENT

All data relevant to the study are included in the article.

ORCID

Hongcui Cao  <http://orcid.org/0000-0002-6604-6867>

Lanjuan Li  <http://orcid.org/0000-0001-6945-0593>

REFERENCES

1. Pallerla SR, Harms D, John R, et al. Hepatitis E virus infection: circulation, molecular epidemiology, and impact on global health. *Pathogens*. 2020;9(10):856.
2. Kamar N, Dalton HR, Abravanel F, Izopet J. Hepatitis E virus infection. *Clin Microbiol Rev*. 2014;27(1):116-138.
3. Fenaux H, Chassaing M, Berger S, Gantzer C, Bertrand I, Schvoerer E. Transmission of hepatitis E virus by water: an issue still pending in industrialized countries. *Water Res*. 2019;151:144-157.
4. Khuroo MS, Khuroo MS, Khuroo NS. Transmission of hepatitis E virus in developing countries. *Viruses*. 2016;8(9):253.
5. Kamar N, Izopet J, Pavo N, et al. Hepatitis E virus infection. *Nat Rev Dis Primers*. 2017;3(1):1-16.
6. Bernal W, Wendon J. Acute liver failure. *N Engl J Med*. 2013;369(26):2525-2534.
7. Kumar A, Saraswat VA. Hepatitis E and acute-on-chronic liver failure. *J Clin Exp Hepatol*. 2013;3(3):225-230.
8. Wang L, Geng J. Acute hepatitis E virus infection in patients with acute liver failure in China: not quite an uncommon cause. *Hepatology*. 2017;65(5):1769-1770.
9. Blackmore L, Bernal W. Acute liver failure. *Clin Med*. 2015;15(5):468-472.
10. Sarin SK, Kumar A, Almeida JA, et al. Acute-on-chronic liver failure: consensus recommendations of the Asian Pacific Association for the study of the liver (APASL). *Hepatol Int*. 2009;3(1):269-282.
11. Gupta E, Pandey P, Pandey S, Sharma MK, Sarin SK. Role of hepatitis E virus antigen in confirming active viral replication in patients with acute viral hepatitis E infection. *J Clin Virol*. 2013;58(2):374-377.

12. Purdy MA, Khudiyakov YE. The molecular epidemiology of hepatitis E virus infection. *Virus Res.* 2011;161(1):31-39.
13. Zhang A, Sun H, Wang X. Serum metabolomics as a novel diagnostic approach for disease: a systematic review. *Anal Bioanal Chem.* 2012;404(4):1239-1245.
14. Vargas AJ, Harris CC. Biomarker development in the precision medicine era: lung cancer as a case study. *Nat Rev Cancer.* 2016;16(8):525-537.
15. Wishart DS. Emerging applications of metabolomics in drug discovery and precision medicine. *Nat Rev Drug Discov.* 2016;15(7):473-484.
16. Rodriguez-Perez R, Cortes R, Guaman A, et al. Instrumental drift removal in GC-MS data for breath analysis: the short-term and long-term temporal validation of putative biomarkers for COPD. *J Breath Res.* 2018;12(3):036007.
17. Vuckovic D. Current trends and challenges in sample preparation for global metabolomics using liquid chromatography-mass spectrometry. *Anal Bioanal Chem.* 2012;403(6):1523-1548.
18. Theodoridis GA, Gika HG, Want EJ, Wilson ID. Liquid chromatography-mass spectrometry based global metabolite profiling: a review. *Anal Chim Acta.* 2012;711:7-16.
19. Zhang A, Sun H, Wang P, Han Y, Wang X. Modern analytical techniques in metabolomics analysis. *Analyst.* 2012;137(2):293-300.
20. Bell LN, Vuppalaanchi R, Watkins PB, et al. Serum proteomic profiling in patients with drug-induced liver injury. *Aliment Pharmacol Ther.* 2012;35(5):600-612.
21. Gonzalez E, van Liempd S, Conde-Vancells J, et al. Serum UPLC-MS/MS metabolic profiling in an experimental model for acute-liver injury reveals potential biomarkers for hepatotoxicity. *Metabolomics.* 2012;8(6):997-1011.
22. Xiong YH, Xu Y, Yang L, Wang ZT. Gas chromatography-mass spectrometry-based profiling of serum fatty acids in acetaminophen-induced liver injured rats. *J Appl Toxicol.* 2014;34(2):149-157.
23. Wu J, Guo Y, Lu X, et al. Th1/Th2 cells and associated cytokines in acute hepatitis E and related acute liver failure. *J Immunol Res.* 2020;2020:6027361.
24. Yang J, Xue R, Wu J, et al. Prognostic nomogram for patients with hepatitis E virus-related acute liver failure: a multicenter study in China. *J Clin Transl Hepatol.* 2021;000:0-0.
25. Wu J, Huang F, Ling Z, et al. Altered faecal microbiota on the expression of Th cells responses in the exacerbation of patients with hepatitis E infection. *J Viral Hepat.* 2020;27(11):1243-1252.
26. Xie Z, Chen E, Ouyang X, et al. Metabolomics and cytokine analysis for identification of severe drug-induced liver injury. *J Proteome Res.* 2019;18(6):2514-2524.
27. Zhai L, Dai X, Meng J. Hepatitis E virus genotyping based on full-length genome and partial genomic regions. *Virus Res.* 120(1-2):57-69.
28. Liu L, Xiao D, Yu J-H, Shen R, Wang M, Li Q. Clinical course of sporadic acute hepatitis E in a hepatitis B virus endemic region. *Int J Infect Dis.* 2018;70:107-114.
29. Clemmesen JO, Kondrup J, Ott P. Splanchnic and leg exchange of amino acids and ammonia in acute liver failure. *Gastroenterology.* 2000;118(6):1131-1139.
30. Recknagel P, Gonnert FA, Westermann M, et al. Liver dysfunction and phosphatidylinositol-3-kinase signalling in early sepsis: experimental studies in rodent models of peritonitis. *PLoS Med.* 2012;9(11):e1001338.
31. Perez MJ, Briz O. Bile-acid-induced cell injury and protection. *World J Gastroenterol.* 2009;15(14):1677-1689.
32. Sokol RJ, Dahl R, Devereaux MW, Yerushalmi B, Kobak GE, Gumprecht E. Human hepatic mitochondria generate reactive oxygen species and undergo the permeability transition in response to hydrophobic bile acids. *J Pediatr Gastroenterol Nutr.* 2005;41(2):235-243.
33. Chen E, Lu J, Chen D, et al. Dynamic changes of plasma metabolites in pigs with GalN-induced acute liver failure using GC-MS and UPLC-MS. *Biomed Pharmacother.* 2017;93:480-489.
34. den Hartigh LJ. Conjugated linoleic acid effects on cancer, obesity, and atherosclerosis: a review of pre-clinical and human trials with current perspectives. *Nutrients.* 2019;11(2):370.
35. Khosla P, Fungwe TV. Conjugated linoleic acid: effects on plasma lipids and cardiovascular function. *Curr Opin Lipidol.* 2001;12(1):31-34.
36. Zhou J, Li Q, Liu C, Pang R, Yin Y. Plasma metabolomics and lipidomics reveal perturbed metabolites in different disease stages of chronic obstructive pulmonary disease. *Int J Chronic Obstruct Pulm Dis.* 2020;15:553-565.
37. Bonkovsky HL, Guo JT, Hou W, Li T, Narang T, Thapar M. Porphyrin and heme metabolism and the porphyrias. *Compr Physiol.* 2013;3(1):365-401.
38. Xue R, Dong L, Wu H, Liu T, Wang J, Shen X. Gas chromatography/mass spectrometry screening of serum metabolomic biomarkers in hepatitis B virus infected cirrhosis patients. *Clin Chem Lab Med.* 2009;47:305-310.
39. Simillion C, Semmo N, Idle JR, Beyoglu D. Robust regression analysis of GCMS data reveals differential rewiring of metabolic networks in hepatitis B and C patients. *Metabolites.* 2017;7:7.

SUPPORTING INFORMATION

Additional supporting information may be found in the online version of the article at the publisher's website.

How to cite this article: Wu J, Xu Y, Cui Y, et al. Dynamic changes of serum metabolites associated with infection and severity of patients with acute hepatitis E infection. *J Med Virol.* 2022;94:2714-2726. doi:10.1002/jmv.27669